Saint Petersburg
RUSSIA

Injectivity Errors in Simulation of Foam EOR

T. N. Leeftink, C. A. Latooij, and W. R. Rossen
Department of Geoscience and Engineering
Delft University of Technology

Injectivity is a key factor in the economics of foam EOR processes. Poor injectivity of low-mobility foam slows the production of oil and allows more time for gravity segregation of injected gas. The conventional Peaceman equation, when applied in a large grid block, makes two substantial errors in estimating injectivity: it ignores the rapidly changing saturations around the wellbore and the effect of non-Newtonian mobility of foam. When foam is injected in alternating slugs of gas and liquid ("SAG" injection), the rapid increase in injectivity from changing saturation near the well is an important and unique advantage of foam injection. Foam is also shear-thinning in many cases.

We use the method-of-characteristics approach of Rossen et al. (2011), which for the first time resolves both changing saturations and non-Newtonian rheology with great precision near the wellbore, and compare to conventionally computed injectivity using the Peaceman equation in a grid block.

By itself, the strongly non-Newtonian rheology of the "low-quality" foam regime makes a significant difference to injectivity of foam. Thus for continuous injection of foam in this regime, the Peaceman equation underestimates injectivity by a factor of two even for grid blocks as small as 10 m wide, and by a larger factor for realistic grid-block sizes. However, one could estimate this effect using the equation for injectivity of power-law fluids, i.e. without accounting for changing water saturation near the well, without much error.

In SAG processes, however, non-Newtonian rheology is less important than accounting for foam collapse in the immediate near-wellbore region. Averaging water saturation in a large grid block misses this dryout very near the well and the Peaceman equation grossly underestimates the injectivity of gas. We illustrate with examples using foam parameters fit to laboratory data.

Introduction

Enhanced Oil Recovery (EOR) processes employing gas injection (miscible and immiscible solvent or steam injection) can be very efficient in recovering oil where the gas sweeps. Unfortunately, gas injection has poor sweep efficiency (Lake, 1989) because of geological heterogeneity, density differences between gas and oil or water, and viscous instability between the gas and the oil or water it displaces. Foam can address all three causes of poor sweep efficiency (Schramm, 1994; Rossen, 1996).

The economics of any EOR process depends on maintaining sufficient injectivity. Injectivity is especially problematic in foam EOR (see e.g., Namdar Zanganeh and Rossen, 2013). Simply injecting a very-low-mobility fluid can force a reduction in injection rate to avoid fracturing the injection well. Unintended fracturing of the injection well has plagued some foam applications in the field (Martinsen and Vassenden, 1999; Kuehne et al., 1990). Moreover, injection rate is crucial to the ability of foam to overcome gravity override of injected gas (Rossen et al., 2010). The good injectivity of a SAG process, in which gas and surfactant solution are injected as alternating slugs, is a major advantage for this injection method in overcoming gravity override (Shan and Rossen, 2004; Faisal et al., 2009; Kloet et al., 2009). In principle, the best foam process for overcoming gravity override is a SAG process with one large slug of surfactant solution followed by one large slug of gas.

Two issues complicate the correct prediction of injectivity in SAG foam EOR processes in reservoir simulation, and in particular injectivity of the gas slug. First is the reaction of foam to changing water saturation close to the well. Foam dries out and collapses abruptly as water saturation falls below a certain value S_w^* (Khatib et al., 1988; Rossen and Zhou, 1995; Alvarez et al., 2001). This "dry-out effect" means that the mobility of gas increases enormously near the injection well and this greatly increases injectivity. Second, gas in foam is a non-Newtonian fluid, at least in some circumstances (Hirasaki and Lawson, 1986; Falls et al., 1989; Alvarez et al., 2001; Xu and Rossen, 2004). Its shear-thinning properties reduce the pressure gradient near the well, which increases injectivity.

The Peaceman equation (Eq. 1, below) used to describe injectivity in reservoir simulators (Computer Modeling Group, 2006; Schlumberger, 2010) misses both these effects: it assumes a uniform water saturation in the grid block containing the injection well and Newtonian mobility at that saturation. Lake (1989) gives an equation for injectivity of non-Newtonian power-law fluid at uniform saturation, but this equation is not commonly implemented in simulations. Sharma et al. (2010) describe how to adjust the parameters of the Peaceman equation on an ad-hoc basis to account for non-Newtonian mobility in the near-wellbore region. In reality, both effects occur simultaneously: saturation varies with position and time near the well, and mobility at each position may be a non-Newtonian function of superficial velocity at that position. Here we address both issues; for simplicity we address them separately.

Effect of Dry-Out Near the Injection Well

With SAG injection, a Buckley-Leverett shock front forms at the leading edge of the gas bank (Rossen et al., 1999; Shan and Rossen, 2004). At the shock there is an abrupt drop in water saturation and water fractional flow. Figures A3 and A4 in Appendix A show an example. This front is followed by a two-phase spreading wave that extends back to the well, in which foam dries out and collapses. In total, two regions are present; a spreading wave with two-phase flow, and ahead of it flow of liquid only. In our study foam dries out near the well because of water displacement and flow. Evaporation of water into the gas is another mechanism of dry-out and mobility increase near the well, as examined in another study of gas injectivity without foam (Pickup et al., 2012). The effects are much more pronounced with foam, but evaporation may also be an issue for foam.

Our focus is the near-wellbore area, so we assume that surfactant concentration is uniform and constant in the water phase as a result of earlier surfactant injection. We model injectivity during gas injection in a SAG process in two ways. First we represent the region of interest as a grid block, as in

reservoir simulators (Computer Modeling Group, 2006; Schlumberger, 2010; Sharma et al., 2012). The injection pressure is calculated from the Peaceman equation, which assumes a cylindrical geometry for a rectangular shaped grid block. Second, we use the Method of Characteristics (MOC) to examine saturation and mobility near the well and overall injectivity in the same region. We use this analytical theory to check the accuracy of the Peaceman equation. Both models are described in the next section.

Assumptions

The following assumptions are made for both cases (grid-block calculation using the Peaceman equation and MOC):

1. All phases are incompressible, as is the reservoir, and components are soluble in only one phase.
2. The reservoir has isotropic and uniform permeability.
3. The surfactant concentration C_s is uniform and constant in the region of interest.
4. There are only two phases flowing, though a third, immobile oil phase may be present. Oil saturation S_o is uniform and constant. For simplicity, we assume here $S_o = 0$.
5. The well radius is r_w. Well skin factor is zero.
6. The reservoir is of uniform height H; the vertical injection well penetrates the entire interval.
7. There are no chemical or biological reactions affecting any of the components.
8. The effect of gravity is negligible in the region of interest.
9. Fluids (in this case, gas) are injected with a constant total volumetric rate Q regardless of injection pressure.
10. Foam properties immediately take their steady-state values corresponding to the local water saturation.

For the first case, in which the region of interest is treated as a grid block, the following assumptions are added to those listed above:

11a. Uniform saturation in the grid block at all times.

12a. For injection-pressure calculations, the reservoir is represented as a cylinder, which is homogeneous and extends from inner radius r_w, where the fluids are injected, to an open boundary at $r_e = W/2$, where W is the width of the (square) grid block. The Peaceman equation applies, with the rectangular grid block approximated as a cylinder:

$$P_w - P_{r_e} = \frac{Q}{2\pi H k \lambda_{rt}} \ln\left(\frac{r_e}{r_w}\right) \quad \text{.....[1]}$$

where Q is injection rate, H formation thickness, k horizontal permeability, and r_e and r_w the radii of the injection well and the edge of the grid block, and total relative mobility λ_{rt} is determined by the average water saturation of the grid block S_w:

$$\lambda_{rt} = \left(\frac{k_{rw}(S_w)}{\mu_w} + \frac{k_{rg}^f(S_w)}{\mu_g}\right) \quad \text{.....[2]}$$

where gas relative permeability k_{rg}^f and viscosity μ_g reflect the effects of foam (see Appendix A).

For the second case where we use the Method of Characteristics, assumptions 1-10 again apply, and in addition

11b. The 1D cylindrical reservoir extends from inner radius r_w, where the fluids are injected, to open outer boundary r_e. Injectivity depends on Darcy's law in radial flow and the variation of water saturation S_w with radial position.

12b. Dispersive processes, including fingering, capillary diffusion and dispersion are negligible.

The foam model used in this study is described in Appendix A.

Case 1: Peaceman Injectivity in Grid Block

In this first case the region of interest is represented as a grid block, either 10 x 10 m or 100 x 100m, surrounding the well. For easier comparison with the MOC calculations below (specifically, to make comparisons at the same dimensionless time), we assume that the grid block has the volume of a cylinder of radius either 5 or 50 m rather than a rectangular volume.

A material balance on the grid block determines how water saturation changes with time. Gas flows in at flow rate Q, and water flows out at rate ($Q\, f_w(S_w)$), yielding

$$\frac{dS_w}{dt} = -\frac{Q\, f(S_w)}{H \pi r_e^2 \varphi} \quad \text{.....[3]}$$

with

$$f_w \equiv \left(1 + \frac{k_{rg}^f(S_w)}{\mu_g} \frac{\mu_w}{k_{rw}(S_w)} \right)^{-1} \quad \text{.....[4]}$$

We express dimensionless time in terms of grid-block pore volumes of gas injected, and dimensionless pressure rise relative to that for water injected into a formation with $S_w = 1$, for which total relative mobility $\lambda_{rt} = 1/\mu_w = 1/(0.001)$ (Pa s)$^{-1}$:

$$t_D = \frac{Qt}{\pi r_e^2 H \varphi} \quad \text{.....[5]}$$

$$P_D = \frac{P_w - P_{re}}{(P_w - P_{re})_{S_w=1}} = \frac{1000}{\lambda_{rt}(S_w)} \quad \text{.....[6]}$$

We solve Eqs. 3 and 1 for dimensionless pressure rise as a function of time numerically. Details are in Leeftink (2013).

Case 2: Solution Using Method of Characteristics

Buckley and Leverett (1941) first applied fractional-flow theory (or, more generally, the Method of Characteristics) to a waterflood. Since then it has proved useful in understanding and improving a variety of EOR processes (Pope, 1980; Lake 1989; Orr, 2007). Here we restrict ourselves to an application to two-phase-flow, i.e. of gas and water. If an oil phase is present, it is immobile, at residual saturation. The assumptions of the theory are listed above. Even with all its assumptions the theory provides valuable insights and proved sufficiently accurate for analysis of a foam field test in the Snorre Field (Martinsen and Vassenden, 1999).

The application of this theory to foam flow is described in detail elsewhere (Zhou and Rossen, 1995; Rossen et al, 1999; Shan and Rossen, 2004). Key to this method is the fractional-flow function $f_w(S_w)$, (Eq. 4). On a plot of this function one first identifies the points representing the injection condition, J, and the initial condition, I; see Figure A3 in Appendix A. In a displacement, saturations between J and I advance through the medium with a dimensionless velocity equal to the slope df_w/dS_w of the fractional-flow function at that saturation. Dimensionless time is defined as in Eq. 5 and dimensionless position in radial flow is

$$x_D = \frac{r^2 - r_w^2}{r_e^2 - r_w^2} \quad \text{.....[7]}$$

where r_w is wellbore radius and r_e is the outer radius of the region of interest, either 5 or 50 m in our case.

A single-valued, continuous solution for $S_w(x_D,t_D)$ requires a monotonically increasing slope from point *J* to point *I* on the $f_w(S_w)$ plot. Otherwise, shocks, i.e. discontinuities in S_w, occur. A material balance on water or gas gives the conditions which have to be satisfied by the shock. Specifically, the shock velocity is equal to the slope of the line linking points on the $f_w(S_w)$ plot upstream and downstream of the shock. The shock velocity must also satisfy the condition of monotonically increasing velocity from the *J* to *I*. Details of the method are in the references above.

The results can be plotted in a time-distance diagram (see Figure A4 in Appendix A), which shows the advance of the characteristics of fixed S_w through the porous medium. Local mobilities along the characteristics plotted in Figure A4 are those at the S_w values with the same slope on the $f_w(S_w)$ curve.

To obtain the rise in injection pressure, one must first convert $S_w(x_D)$ to $S_w(r)$ (Eq. 7) and then integrate for pressure from outer radius r_e to wellbore radius r_w using Darcy's law:

$$\frac{\partial P}{\partial r} = \frac{-Q}{2\pi r H k \lambda_{rt}(S_w(r))} \quad . \quad \text{[8]}$$

We carry this integration out numerically; details are in Leeftink (2013).

Results

Peaceman Injectivity in a Grid Block

Figure 1 shows water saturation in the grid block as a function of dimensionless time t_D. The plot is the same for both grid-block sizes as a function of dimensionless time. Figure 2 shows dimensionless injection pressure as a function of dimensionless time. Again, the plot is the same for both grid-block sizes, because injection pressure is dimensionalized by the injection pressure for water, so that the different ratio of wellbore and grid-block radii (Eqs. 1 and 6) affects both cases identically. Although the period of low injectivity (large P_D) appears brief in Fig. 2, if injection pressure were limiting rather than rate, injection rate would slow down by a factor of several hundred at the peak in P_D, and the period of low injectivity would be greatly prolonged.

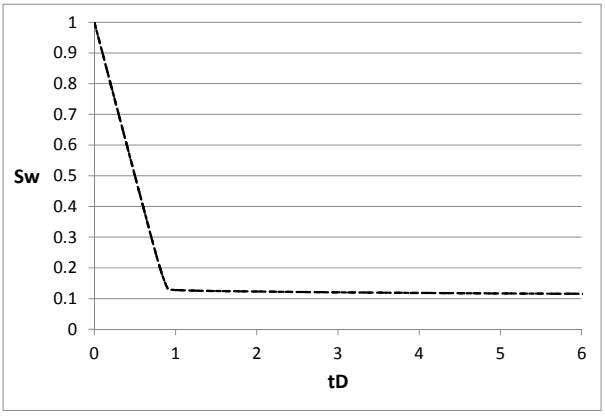

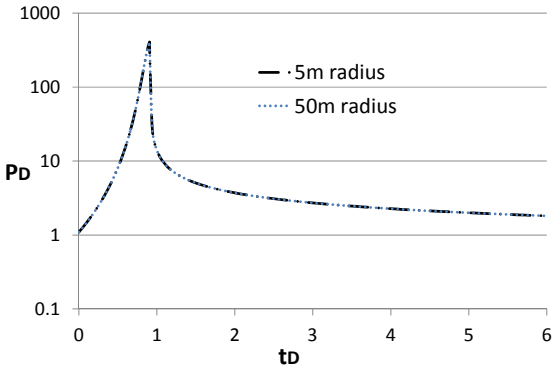

***Figure 1** (left). Water saturation in the grid block as a function of dimensionless time t_D. The plot is the identical for 10-m-wide and 100-m-wide grid blocks.*
***Figure 2** (right). Dimensionless injection pressure as a function of dimensionless time. The plot is the identical for 10-m-wide and 100-m-wide grid blocks.*

Solution Using Method of Characteristics

Figure 3 shows dimensionless injection pressure as a function of dimensionless time for the 10-m and 100-m wide regions. The plots differ because the effect of greater mobility near the wellbore is different for the two cases. For the 100-m wide grid block the near-wellbore region dries out in a smaller faction of the time it takes to inject a pore volume of gas. For gas injection in SAG, injectivity

is least near the start of gas injection, when the low-mobility front of the gas bank is near the well and still there is water to displace at larger radii. With increasing time mobility rises near the well (Fig. A4) and injectivity increases.

Figure 4 compares P_D calculated using the Peaceman equation and assuming uniform saturation in the grid block with that calculated using the MOC for the two grid-block sizes. For a short time, injectivity is less than estimated using the Peaceman equation, but soon, and for the rest of the period of gas injection, the Peaceman equation grossly underestimates injectivity. The comparison is less extreme in this case than if we had used a foam model where foam collapses completely at the well and mobility there rises by another factor of 10 to about 50,000 $(Pa\ s)^{-1}$; see Appendix A.

If injection pressure is fixed rather than injection rate, Figs. 2 and 4 greatly understate the injectivity problem with the Peaceman equation in a grid block that is assumed to have uniform saturation. If injection pressure is fixed, then injection rate scales with $(1/P_D)$, and the advance of physical time scales like the integral of (P_D) with respect to t_D. The physical time required to inject a grid-block pore volume of gas is shown in Figs. 5 and 6. A unit of time on these plots corresponds to the time it would take to inject one grid-block pore volume of water with 100% water saturation in the grid block. It takes about 42 time units to inject a grid-block pore volume of gas using the Peaceman equation (for either grid-block size), compared to 1.12 and 1.57 time units for grid blocks of 50-m and 5-m radius, calculated with the MOC.

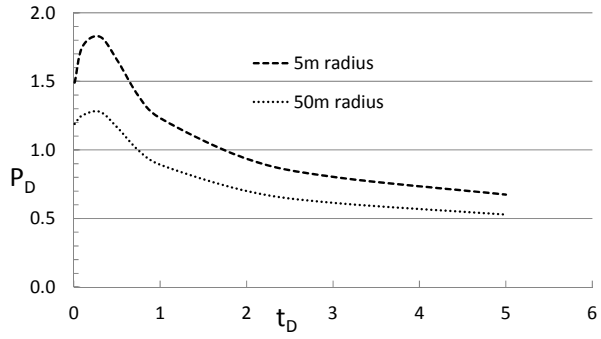

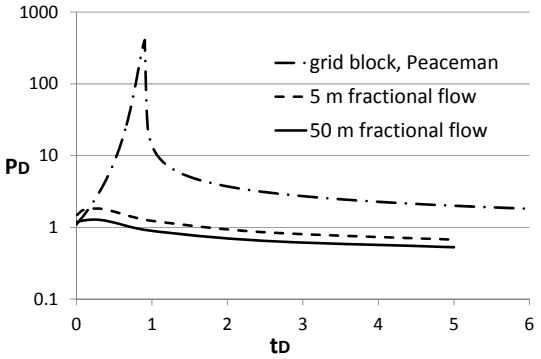

***Figure 3** (left). Dimensionless injection pressure as a function of dimensionless time t_D based on fractional-flow solution for the two grid-block sizes.*
***Figure 4** (right). Comparison of dimensionless injection pressure computed using the Peaceman Equation and the solution using the MOC, which accounts for lower water saturation near the well.*

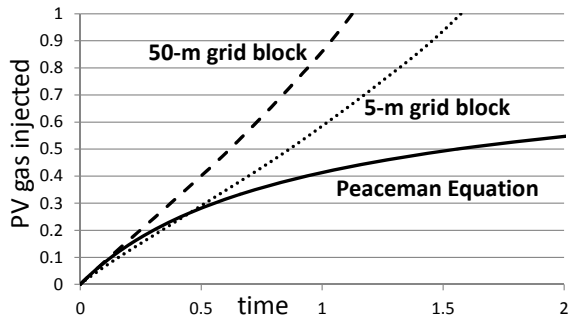

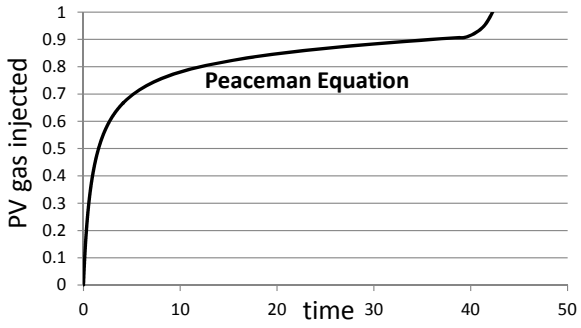

***Figure 5** (left). Cumulative injection in terms of grid-block pore volume of gas: MOC solution for 5-m and 50-m radii and Peaceman Equation (which gives same solution for either grid-block size). One unit of time here represents time it would take to inject one grid-block pore volume of water with 100% water saturation in the grid block.*
***Figure 6** (right). Extended plot of behavior computed with Peaceman equation for longer times.*

Injectivity is so greatly underestimated by the Peaceman equation in a grid block because S_w in the grid block must pass through all the extremely low mobilities between the injected and initial

saturations (Fig. A2). In reality, upon gas injection there is a shock front past the saturations of lowest mobility, as illustrated by the MOC solution. Everywhere throughout the foam bank in Fig. A4 the mobility is at least 93 times greater than at its minimum in Fig. A2.

Effect of Non-Newtonian Viscosity

Rossen et al. (2011) describe a method for modeling 1D dynamic two-phase displacements with non-Newtonian phase viscosities using the method of characteristics (MOC). Unlike the model in the previous section, for non-Newtonian fluids the characteristics are curved, and computation of the velocity of the shock front at the leading edge of the foam bank is complex. Rossen et al. show that, for SAG injection, a simple numerical solution using the MOC is possible behind the shock front, i.e. in the near-wellbore region. Although the method employs a numerical solution of equations derived from the MOC, these equations can be solved to an arbitrary level of precision, much more accurately than is feasible with conventional simulation. To simplify the model and focus on non-Newtonian effects, Rossen et al. (2011) excluded the effect of water saturation on foam stability, specifically the abrupt collapse of foam at a limiting water saturation S_w^* described in the previous section. Thus their study includes the simultaneous effects of changing water saturation and non-Newtonian viscosity, but it excludes by far the largest effect of changing water saturation in a SAG process, the dry-out effect. In a SAG process foam is in the "high-quality" regime dominated by dry-out; rheology in this regime can be non-Newtonian (Alvarez et al., 2001), but modeling this effect would require making S_w^* a function of superficial velocity. This is allowed in the current STARS foam simulator (Coombe, 2012) but is not frequently used in simulation.

In the foam model of Rossen et al. (2011), gas mobility is reduced by foam by a factor that is independent of water saturation but depends on total superficial velocity like a power-law fluid with power-law exponent ½. Mobility depends on water saturation weakly because of the dependence of foam-free relative permeabilities of water and gas on water saturation. Values of mobility below correspond to "effective viscosity" of foam (inverse mobility relative to that of water in single-phase flow) of 24 to 530 cp. Our focus is not on the magnitude of injection pressure-rise, which is extraordinary given the low mobility of the foam here, but on the effect of non-Newtonian foam behavior on it. Details of the foam model are in Appendix B.

Rossen et al. (2011) note that an important implication of this model is the effect on injectivity, but do not calculate injectivity. In this paper we use the results of Rossen et al. for water saturation as a function of time and radial position to determine injectivity for shear-thinning foam in a SAG process. We integrate for pressure around the well numerically using the positions of the characteristics at the given time, as in Eq. 8, but with λ_{rt} dependent on both S_w and position r. Details of the calculations are in Latooij (2012). The definitions of dimensionless time and injection pressure are the same as in Eqs. 5 and 6. As above, the wellbore radius is 0.1 m, and the outer radii are either 5 or 50 m. For a radius of 5 m, Fig. 7 shows water saturation around the well at a dimensionless time $t_D = 10$.

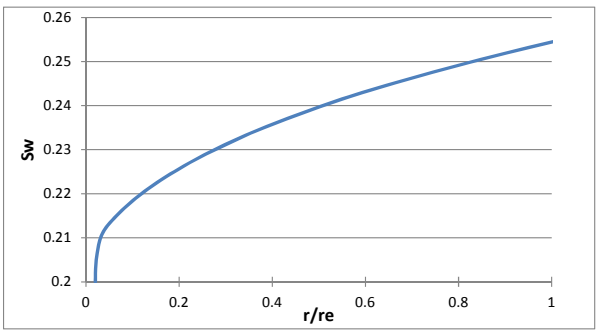

Figure 7. *Water saturation around the well at dimensionless time $t_D = 10$, long after the shock has passed beyond the region of interest; 10-m-wide grid block.*

Results

We compute injectivity at two times, one shortly after the shock at the leading edge of the foam bank has left the region of interest ($t_D = 1$), and again at ten times this time ($t_D = 10$). For a 10-m wide grid block (outer radius 5 m), at $t_D = 1$,the dimensionless injection pressure P_D is 87, reflecting the extremely strong foam assumed in this section (Appendix B). If however one used the Peaceman equation with the total relative mobility equal to that at r = 5 m at this time, the dimensionless rise would have been 210, i.e. 2.41 times larger. Ten times later, at $t_D = 10$, the dimensionless rise in injection pressure is 83, again reflecting an extremely strong foam. If however one used the Peaceman equation with the total relative mobility equal to that at r = 5 m, the dimensionless rise would have been 190, i.e. 2.29 times larger.

We distinguish the effects of shear-thinning rheology and changing water saturation at the well as follows. First we examine the effect of non-Newtonian (shear thinning) rheology alone. In this case we allow that the effective viscosity changes with radial distance, but assume S_w is uniform throughout the entire region and is equal to its value at the well, i.e. 0.2. The total relative mobility λ_{rt} then depends only on radial position (Eq. B3). At the well ($x_D = 0$) we find that $\lambda_{rt} = 42.23$ (Pa s)$^{-1}$ (an effective viscosity of 23 cp) whereas at the outer radius $\lambda_{rt} = 5.97$ (Pa s)$^{-1}$ (effective viscosity 167 cp). The total relative mobility is a factor of 7 lower at the wellbore compared to that at r = 5 m. As shown above, the result is injectivity over twice as large as that estimated using the mobility at the outer radius.

Next we allow for nonuniform water saturation but not non-Newtonian rheology. At $t_D = 1$, at r = 5 m $S_w = 0.31$ and at the wellbore $S_w = 0.2$. Excluding the non-Newtonian effects, the difference in total relative mobility at these two saturations is only 25%. At $t_D = 10$, the difference in mobilities is about 13%. Thus, in this case, with foam dry-out excluded, the effect of changing water saturation near the well is much less important than shear-thinning viscosity.

These results show that although the changing water saturation does have an impact on injectivity in this model (13 to 25%), the effect of shear thinning-rheology on injectivity is much greater (i.e., by a factor of more than 2) and is therefore the more important effect. Moreover, as grid-block size increases, the effect of shear thinning on injectivity increases.

For a 100-m wide grid block (outer radius 50 m), at $t_D = 1$ dimensionless rise in injection pressure is 183. If however one used the Peaceman equation with the total relative mobility equal to that at r = 50 m, the dimensionless rise would have been 618, i.e. 3.38 times larger. At $t_D = 10$, the dimensionless rise in injection pressure is 177. If however one used the Peaceman equation with the total relative mobility equal to that at *r* = 50 m, the dimensionless rise would have been 576, i.e. 3.26 times larger. As for the 10-m wide grid block, the effect of S_w alone in this case is much smaller: about a 17% difference in mobility at $t_D = 1$, and 9% at $t_D = 10$. The total relative mobility at the injection wellbore is 22 times greater than that at 50 m for both $t_D = 1$ and 10.

Although in this case the effect of dry-out is much greater than that of non-Newtonian mobility, the effect of non-Newtonian mobility is still significant; ignoring it would lead to significant errors in computed injectivity.

Conclusions

The following conclusions relate to the dry-out effect on foam and foam injectivity:

1. In simulation of gas injection in SAG processes, the Peaceman equation, combined with an assumption of uniform saturation in the injection-well grid block, can lead to a massive underestimation of true gas injectivity. If injection pressure is limiting, the period of incorrectly calculated poor injectivity can last for long times. In our example, using the Peaceman equation, the injection-well grid block at one point experiences mobility (Fig. A2) almost 100 times lower than that anywhere within the foam bank (Fig. A4).

2. These results are expressed in dimensionless time based on grid-block pore volume. Reducing grid size around the injection well would reduce the duration of the effect on the reservoir scale, at the price of slower simulator execution.
3. The foam model used here assumes (Fig. A1) that gas mobility is reduced by over a factor of 10 even at irreducible water saturation S_{wr}. If instead foam collapsed completely at S_{wr} and gas mobility at the well were 10 times greater, the contrast between true behavior and that simulated using the Peaceman equation would be even greater.

The following conclusion relates to the effect of non-Newtonian foam behavior and injectivity:

4. Non-Newtonian foam mobility is important to foam injectivity. In the example shown, the actual injectivity is about 2.3 and 3.3 times lower than that which would be estimated using the Peaceman equation and the mobility at the outer radius, for 10-m and 100-m grid blocks, respectively. If one excludes the dry-out effect, then the effect of changing saturation on this result is relatively small.

References

Alvarez, J. M., Rivas, H., and Rossen, W. R., "A Unified Model for Steady-State Foam Behavior at High and Low Foam Qualities," *SPE Journal* **6** (Sept. 2001), 325-333.

Buckley, S. E., and Leverett, M. C., "Mechanism of Fluid Displacement in Sands," *Trans. AIME* **146** , 107-116 (1941).

Cheng, L., Reme, A. B., Shan, D., Coombe, D. A. and Rossen, W. R., "Simulating Foam Processes at High and Low Foam Qualities," paper SPE 59287 presented at the 2000 SPE/DOE Symposium on Improved Oil Recovery, Tulsa, OK, 3-5 April.

Computer Modeling Group, *STARS User's Guide*, Version 2006, Calgary, Alberta, Canada.

Coombe, D. A., personal communication (2012).

Faisal, A., Bisdom, K., Zhumabek, B., Mojaddam Zadeh, A., and Rossen, W. R., "Injectivity and Gravity Segregation in WAG and SWAG Enhanced Oil Recovery," SPE 124197 presented at the 2009 SPE Annual Technical Conference and Exhibition held in New Orleans, Louisiana, USA, 4–7 October 2009.

Falls, A. H., Musters, J. J. and Ratulowski, J., "The Apparent Viscosity of Foams in Homogeneous Bead Packs", *SPE Reserv. Eng.* **4** (May 1989), 155-164

Hirasaki, G. J., and Lawson, J. B., "Mechanisms of Foam Flow Through Porous Media - Apparent Viscosity in Smooth Capillaries," *SPE J* **25**, 176-190 (1985).

Khatib, Z. I., Hirasaki, G. J. and Falls, A. H., "Effects of Capillary Pressure on Coalescence and Phase Mobilities in Foams Flowing through Porous Media", *SPE Reserv. Eng.* **3** (August 1988), 919-926.

Kloet, M. B., Renkema, W. J., and Rossen, W. R., "Optimal Design Criteria for SAG Foam Processes in Heterogeneous Reservoirs," SPE 121581 presented at the 2009 SPE EUROPEC/EAGE Annual Conference and Exhibition, Amsterdam, The Netherlands, 8–11 June 2009.

Kuehne, D. L., Ehman, D. I., Emanuel, A. S., and Magnani, C. F., "Design and Evaluation of a Nitrogen-Foam Field Trial," *J. Petr. Techol.* **42**, 504-512 (1990).

Lake, L. W., *Enhanced Oil Recovery*, Prentice Hall, Englewood Cliffs, New Jersey, USA (1989).

Latooij, C. A., "Injectivity in Non-Newtonian Two-Phase Flow," BSc thesis BTA/PE/12-18, Delft University of Technology, 2012; available at http://repository.tudelft.nl/.

Leeftink, T. N., "Injectivity errors in simulation of foam EOR," BSc thesis, Delft University of Technology, in progress (2013); obtainable from http://repository.tudelft.nl/.

Martinsen, H. A. and Vassenden, F., "Foam-Assisted Water Alternating Gas (FAWAG) Process on Snorre," presented at the 1999 European IOR Symposium, Brighton, U.K., 18–20 August.

Namdar Zanganeh, M., Kam, S. I., LaForce, T. C., and Rossen, W.R., "The Method of Characteristics Applied to Oil Displacement by Foam," *SPE Journal* **16**, 8-23 (2011).

Namdar Zanganeh, M., and Rossen, W. R., "Optimization of Foam EOR: Balancing Sweep and Injectivity," accepted for publication in *SPE Reservoir Evaluation and Engineering* (2013).

Orr, F. M., *Theory of Gas Injection Processes*, Tie-Line Publications (2007).

Pickup, G. E., Jin, M., and Mackay, E.J., "Simulation of Near-Well Pressure Build-up in Models of CO2 Injection," paper B34 presented at the European Conference on the Mathematics of Oil Recovery, Biarritz, France, 10-13 September 2012.

Pope, G. A., "The Application of Fractional Flow Theory to Enhanced Oil Recovery," *SPE J* **10**, 191–205. (1980).

Rossen, W. R., "Foams in Enhanced Oil Recovery," in R. K. Prud'homme and S. Khan, ed., *Foams: Theory, Measurements and Applications*, Marcel Dekker, New York (1996), pp. 413-464.

Rossen, W. R., van Duijn, C. J., Nguyen, Q. P., Shen, C., and Vikingstad, A. K., "Injection Strategies to Overcome Gravity Segregation in Simultaneous Gas and Water Injection Into Homogeneous Reservoirs," *SPE Journal* **15**, 76-90 (2010).

Rossen, W. R., Venkatraman, A., Johns, R. T., Kibodeaux, K. R., Lai, H., and Moradi Tehrani, N., "Fractional Flow Theory Applicable to Non-Newtonian Behavior in EOR Processes," *Transport in Porous Media* **89**(2), 213-236 (2011).

Rossen, W. R., Zeilinger, S. C., Shi, J.-X., and Lim, M. T., "Simplified Mechanistic Simulation of Foam Processes in Porous Media," *SPE Journal* **4**, 279-287 (Sept. 1999).

Rossen, W. R. and Zhou, Z. H., "Modeling Foam Mobility at the Limiting Capillary Pressure," *SPE Adv. Technol.* **3**, 146-152 (1995).

Schlumberger, *ECLIPSE* Reservoir Simulation Software, Version 2010.2, Technical Description*, 2010.

Schramm, L. L. (ed.) *Foams: Fundamentals and Applications in the Petroleum Industry*, ACS Advances in Chemistry Series No. 242, Am. Chem. Soc., Washington, DC (1994).

Sharma, A., Delshad, M., Huh, C., and Pope, G. A., "A Practical Method to Calculate Polymer Viscosity Accurately in Numerical Reservoir Simulators," SPE 147239 presented at the SPE Annual Technical Conference and Exhibition held in Colorado, Denver, USA, 31 October 2011–2 November 2010.

Shan, D. and Rossen, W. R., "Optimal Injection Strategies for Foam IOR," *SPE Journal* **9**, 132-150.

Xu, Q. and Rossen, W. R., "Dynamic Viscosity of Foam in Porous Media," Proc. EuroConference on Foams, Emulsions and Applications, Delft, The Netherlands, 5-8 June 2000.

Zhou, Z. H. and Rossen, W. R,. "Applying Fractional-Flow Theory to Foam Processes at the 'Limiting Capillary Pressure'," *SPE Adv. Technol.* **3**, 154-162 (1995).

Appendix A. Foam Model Used in Study of Effect of Dry-Out

In the absence of foam we use the following relative-permeability functions for water and gas:

$$k_{rw} = 0.6822\left(\frac{S_w - 0.05}{0.90}\right)^{2.6844} \quad \text{[A1]}$$

$$k_{rg}^{o} = 0.8649\left(\frac{0.95 - S_w}{0.90}\right)^{2.2868} \quad \text{[A2]}$$

where the superscript ^{o} indicates that this is the relative permeability in the absence of foam. Water and gas viscosities 1.0 and 0.02 cp (0.001 and 0.00002 Pa s), respectively. With foam, the water relative-permeability function and viscosity are not altered but gas mobility is greatly reduced (Rossen, 1996). Here we use the foam model in STARS™ (Cheng et al. 2000), in which the effect of foam is represented by an alteration in gas relative permeability.

$$k_{rg}^{f} = \frac{k_{rg}^{o}(S_w)}{1 + fmmob\left(0.5 + \frac{\arctan(epdry*(S_w - fmdry))}{\pi}\right)} \quad \text{[A3]}$$

Parameter fmmob is the reduction in gas mobility for full-strength foam, in the "low-quality" or wet regime, fmdry the water saturation at the transition to the "high-quality regime," where foam dry-out dominates behavior, and epdry is a parameter that governs the abruptness of this transition. Here we

choose fmmob = 34,000, fmdry = 0.13, and epdry = 10,000. These values are similar to those Cheng et al. (2000) derived from coreflood data. Figure A1 shows gas and water relative-permeability functions with these parameters, and Fig. A2 shows total relative mobility (Eq. 2) as a function of water saturation for those parameters. Total relative mobility in Fig. A2 is inversely related to effective viscosity of foam; $\lambda_{rt} = 10$ corresponds to an effective viscosity of 100 cp. For single-phase gas flow (at $S_w = S_{wr} = 0.05$), $\lambda_{rt} = 43{,}250$. Figure A3 shows the fractional-flow curve (Eq. 4) for this foam model, along with the shock at the leading edge of the foam bank, and Fig. A4 shows the time-distance diagram for the process, with total relative mobilities marked in for several characteristics.

Note that even at irreducible water saturation S_{wr} gas mobility is reduced by a factor of more than 10 by foam according to this model (Fig. A1). One expects (Khatib et al., 1988) that foam has collapsed at the large capillary pressure at S_{wr}. If the model represented this accurately, mobility at the wellbore would be 43,250 instead of 4,301 as in Fig. A4. The failure of the foam model in STARS to give complete foam collapse at S_{wr} has a large impact on mobility in SAG displacements (Namdar Zanganeh et al., 2011), and, as shown here, on injectivity.

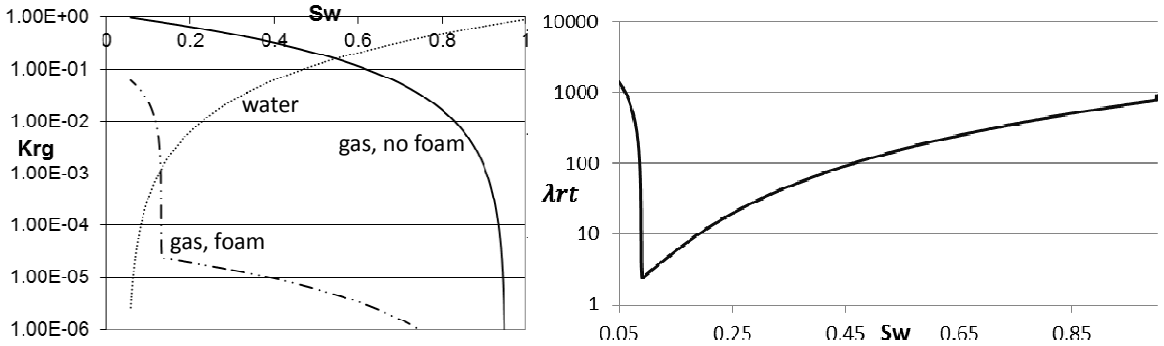

Figure A1 *(left). Gas and water relative-permeability functions for the study of foam dry-out.*
Figure A2 *(right). Total relative mobility of foam (Pa s)$^{-1}$ as a function of water saturation for the study of foam dry-out.*

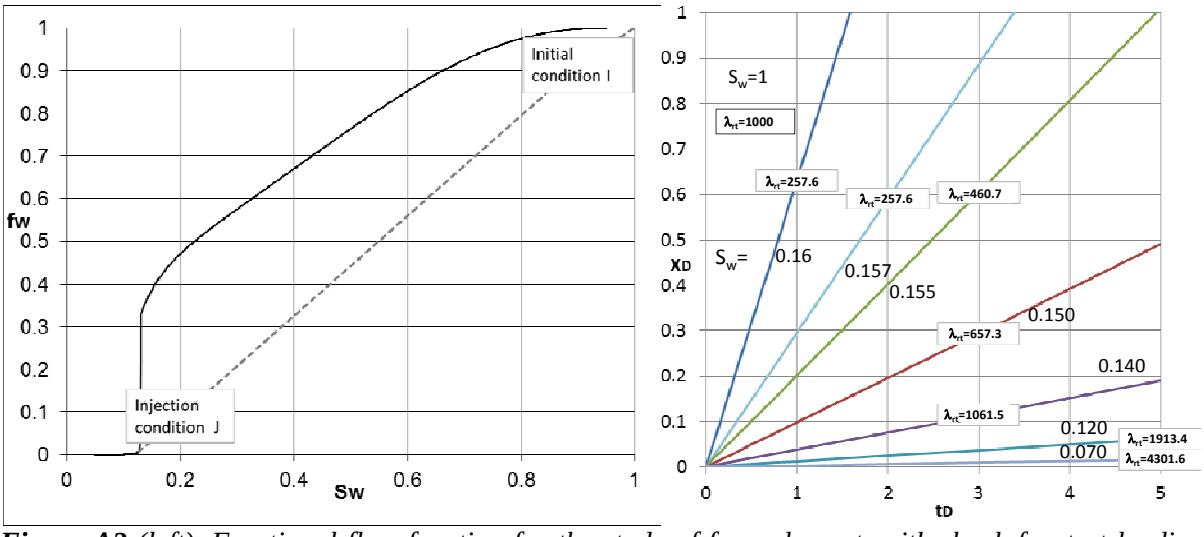

Figure A3 *(left). Fractional-flow function for the study of foam dry-out, with shock front at leading edge of gas bank drawn in.*
Figure A4 *(right). Time-distance diagram for gas injection in study of foam dry-out. Boxed values are total relative mobility (Pa s)$^{-1}$ for the given characteristic, except (upper left) for 1000, the total relative mobility of the initial state (to the left of the steepest characteristic, which is also the shock front).*

Appendix B. Foam Model Used in Non-Newtonian Injectivity Calculations

In this case we take the relative permeabilities used by Rossen et al. (2011), i.e.

$$k_{rw} = 0.2\left(\frac{S_w - 0.2}{0.6}\right)^{4.2} \quad \text{[B1]}$$

$$k_{rg}^{o} = 0.657\left(\frac{0.8 - S_w}{0.6}\right)^{1.3} \quad \text{[B2]}$$

Water and gas viscosities in the absence of foam are 0.001 and 0.00002 Pa s as in the dry-out study. Foam does not affect water relative permeability or viscosity, but does greatly affect gas mobility. It is equivalent to describe this effect as an effect on relative permeability or viscosity. Described as an effect on gas relative permeability we use

$$k_{rg}^{f} = \frac{k_{rg}^{o}(S_w)}{55000\left(\frac{r}{500}\right)^{(1-n)/2}} = \frac{0.657\left(\frac{0.8 - S_w}{0.6}\right)^{1.3}}{55000\left(\frac{r}{500}\right)^{(1-n)/2}} \quad . \quad \text{[B3]}$$

This corresponds to a foam with extremely large mobility reduction (by a factor of 55,000, which is similar to the model fit of Cheng et al. (2000) to laboratory data without oil) at a radial distance of 500 m, and with the mobility reduction scaling like a power-law fluid with exponent *n* for shorter distances. We assume a power-law exponent of ½. Thus at the wellbore radius of 0.1 m gas mobility is reduced by a factor of 6,540 and at a distance of 1 m by a factor 11,631. The relatively small value of power-law exponent *n* here (½) is similar to behavior observed in the “low-quality" foam regime (Alvarez et al., 2001) i.e., far from the dry conditions of foam collapse. Like Rossen et al. (2011) we assume a particularly simple foam model here to illustrate the effects of shear-thinning rheology without the other complications of foam behavior.